International Journal of Engineering Research
Volume No.4, Issue No.8, pp : 456-464
ISSN:2319-6890)(online),2347-5013(print)
01 August 2015

Smart Energy Management controller for a Micro Grid

Atef. M. Mansour*, Khaled .N. Faris*, Essam El-Din Aboul Zahab**
* Electronics research institute. Dokki, Giza, Egypt
** Faculty of engineering, Cairo University. Giza, Egypt
Atef_mohamed52@yahoo.com, khalederi@yahoo.com, zahab0@yahoo.com

Abstract: ***This paper adopts a proposed energy management controller in a micro grid. This micro grid integrates both a renewable energy source and energy storage systems. Photovoltaic (PV) is adopted as a main power source, a valve regulated lead acid battery, and Super-capacitor are the energy storage system. This hybrid energy storage integrates the advantages of a high energy density of the battery and a high power density of the super-capacitor to decrease the stress on the battery and to decrease the voltage change at transient conditions. The proposed controller consists of two control units. The First unit is used for maximum power point tracking (MPPT), and the Second is used to drive the bidirectional converters for charging and discharging modes of the battery and the super capacitor; according to the load demand and the environmental conditions. The simulation results show the effectiveness and the efficiency of the proposed control strategy.***

Keywords— Photovoltaic (PV), MPPT, Fuzzy logic controller (FLC), Energy Storage System (ESS), Energy management controller.

I. Introduction

Micro grids are very interesting to decrease the environmental impacts of fossil fuel by increasing the penetration of renewable energy sources. It can be connected to the utility or operated as a standalone micro grid [1, 2]. In this paper a model of a simple micro grid is adopted. The main power source in the adopted micro grid is a PV source. The output power of the PV is greatly affected by the environmental conditions so that it is necessary to have energy storage. Generally valve regulated lead acid (VRLA) battery is the most common energy storage technology working in standalone systems because of its low cost and wide availability [3]. The batteries have high energy density so that it can supply the load for long time. The disadvantage of the battery is the short life cycle, and a short shelf storage and leakage of stored energy. This is because of the basic nature of chemical reactions of a battery. On the other hand super capacitor (SC) has the advantages of fast charge and discharge of energy and a longer life cycle, because of electrostatic nature of. The SC can be charged and discharged more than one million times [4]. Therefore battery-supercapacitor hybrid ESS will take advantages of both technologies and provide high power and energy density as shown in Fig. 1 [5]. So that the adopted micro grid integrates PV source, battery and SC as shown in Fig. 2.

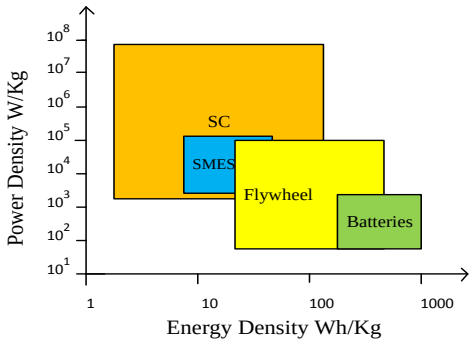

Fig. 1. Power density versus energy density ranges for different energy storage systems.

In this paper a modified perturb and observe (P&O) MPPT algorithm is introduced and compared with FLC based MPPT. Also an energy management controller is proposed. This controller is responsible for stabilizing the output voltage at the reference voltage by controlling the power flow from PV to the load and controlling charging or discharging the energy storage systems. This paper includes seven parts as following: part one (I) is the introduction, part (II) is the system configuration, part (III) includes modelling of the system components, part (IV) includes the control strategy, part (V) includes simulation results, part (VI) includes experimental case study, part (VII) includes conclusions.

II. System Configuration

The micro grid system integrates Istar Solar photovoltaic module, battery pack of two batteries battery and supercapacitor module and a DC load. Table1 shows the nominal parameters of these micro grid components. Fig. 2 shows the micro grid configuration. The PV panel connected to the DC Bus through the boost converter. The battery connected to the DC bus through the bidirectional buck boost converter. The SC connected to the DC Bus through a bidirectional buck boost converter. In this study we will simulate different configurations of this micro grid system as following: 1) The micro grid with PV source, 2) The micro grid with PV source and battery, 3) The micro-grid with PV, battery and SC.

TABLE 1. Nominal parameters of the micro grid components

PV module@ STC	P_{max} = 300 W, V_{max}= 37.6 V, I_{max}=7.98 A
Two series Batteries	Valve regulated Lead acid 12 V, 50 Ah
Supercapacitor	83 Farad, 48 V

ISSN:2319-6890)(online),2347-5013(print)
01 August 2015

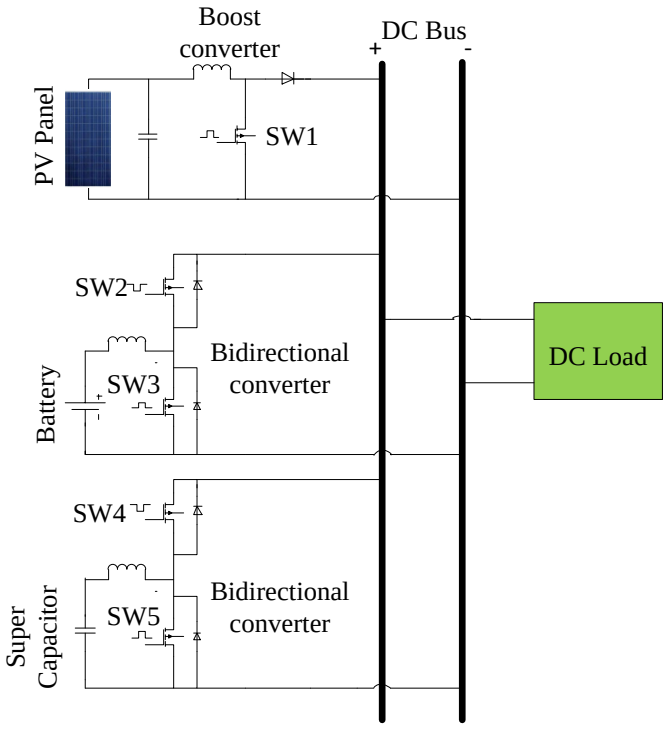

Fig. 2. Adopted micro grid

III. Modelling of the system components

A. PV model

The PV cell can be modelled by a current source in parallel with a diode [9]. As shown in Fig. 3.

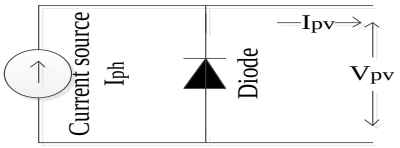

Fig. 3. PV cell.

The electrical characteristics of the PV cell are nonlinear and vary according to the solar insolation (G) and the cell temperature (T). The output current Ipv can be expressed by equation 1

$$I_{pv} = I_{ph} - I_0[exp\ (\frac{Q.V_{pv}}{A.k.T}) - 1] \quad (1)$$

Where I_{pv} is the output current from the PV cell, I_{ph} is the photo generated current, I_0 is the dark saturation current, Q is the electron charge $=1.6*10^{-19}$ (C), V_{pv} is the output voltage of the PV cell, A is the ideality factor of the diode, K is Boltzmann constant $=1.38*10^{-23}$ (J/K), T is the cell temperature (^oC). The output current of a PV module integrates a number of cells connected in series (N_s) and number of cells connected in parallel (N_p) can be expressed by equation 2. The simulated electrical characteristics of the adopted PV module are shown in Fig. 4.

$$I_{pv} = N_p.I_{ph} - N_p.I_0[exp\ (\frac{Q.V_{pv}}{N_s.A.k.T}) - 1] \quad (2)$$

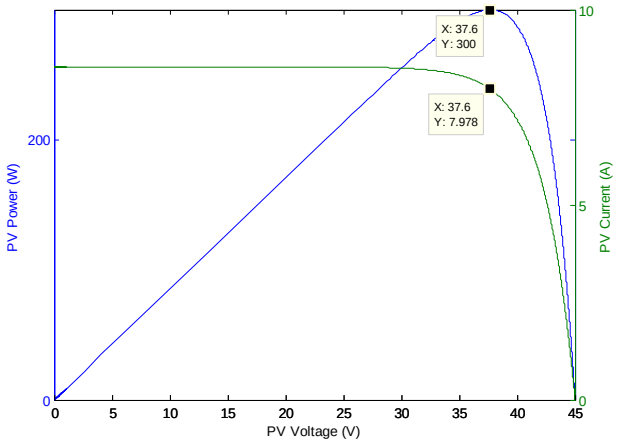

Fig. 4. Simulated electrical characteristics of IS4000P PV module.

B. Battery model

The equivalent circuit of a generic battery dynamic model parameterized to represent most popular types of rechargeable batteries. This model can be represented by a simple controlled voltage source in series with a constant resistance, as shown in Fig. 5 [10].

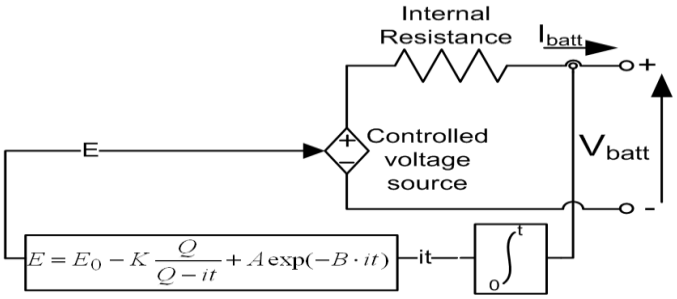

Fig. 5. Generic model of battery.

$$E = E_0 - K\frac{Q}{Q - \int idt} + A\exp(-B.\int idt) \quad (3)$$

$$V_{batt} = E - i.R \quad (4)$$

Where, E is no-load voltage (V), E0 is battery constant voltage =12V, K is polarization voltage (V), Q is battery capacity (Ah), ∫ idt is the actual battery charge (Ah), A is the exponential zone amplitude (V), B is the exponential zone time constant inverse $(Ah)^{-1}$, V_{batt} is the battery voltage (V), R is the internal resistance (ohm), i is the battery current (A).

C. Super capacitor model

In this simulation study a supercapacitor module Maxwell BMOD0083-P048 is used. The generic model of supercapacitor shown in Fig. 6 is adopted in this study [11].

ISSN:2319-6890)(online),2347-5013(print)
01 August 2015

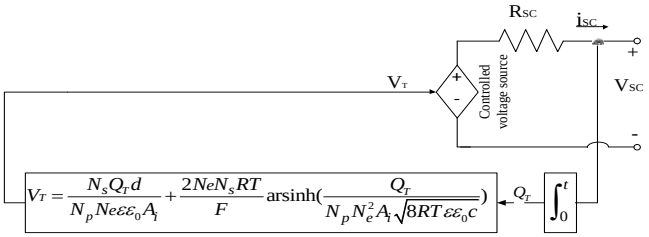

Fig. 6. Generic model of SC.

The SC module has a number of SC cells connected in series Ns and a number of SC cells connected in parallel Np. The output voltage can be obtained using equation 5 as following:

$$V_{SC} = \frac{Q_T}{C_T} - i_{SC}.R_{SC} \quad (5)$$

where

$$Q_T = N_p Q_c = \int i_{SC} dt \quad (6)$$

$$C_T = \frac{N_p}{N_s}.C \quad (7)$$

$$C = \left[\frac{1}{C_H} + \frac{1}{C_{GC}}\right]^{-1} \quad (8)$$

$$C_H = \frac{N e \varepsilon \varepsilon_0 A_i}{d} \quad (9)$$

$$C_{GC} = \frac{F Q_c}{2 N_e RT}\sinh\left(\frac{Q_c}{N_e^2 A_i \sqrt{8RT\varepsilon\varepsilon_0 c}}\right) \quad (10)$$

Where V_{sc} supercapacitor output voltage (V), Q_T is the total electric charge (C), i_{SC} is the SC current (A), R_{SC} is the resistance of SC module (ohm), Q_c is the electric charge of one SC cell (C), C is the capacitance of SC cell (farads), C_H is the Helmholtz capacitance (farads), C_{GC} is the Gouy-Chapman capacitance (farads), N_e is the number of electrode layers, ε and ε_0 are the permittivity of electrolyte material and free space respectively (F/m), A_i is the interfacial area between the electrodes and the electrolyte (m^2), d is the molecular radius (m), F is Faraday constant = 96485.3383, R is the ideal gas constant = 8.314472, T is the operating temperature in kelvin, c is the molar concentration (mol . m^{-3}). The parameters of the SC are fed to the model as follow, rated voltage = 48 V, rated capacitance = 83 F, equivalent series resistance = 0.01 ohms, N_s= 18 capacitors, N_p capacitors = 1, leakage current = 0.003A. The simulated discharge current profiles of the model are verified with the discharge current profiles of the supercapacitor data sheet as shown in Fig. 7.

IV. Control Strategy

In this paper the control strategy is divided into two main control units. (1) First control unit responsible for MPPT and (2) second control unit is the energy management control unit Each control unit will be explained in detail as following:

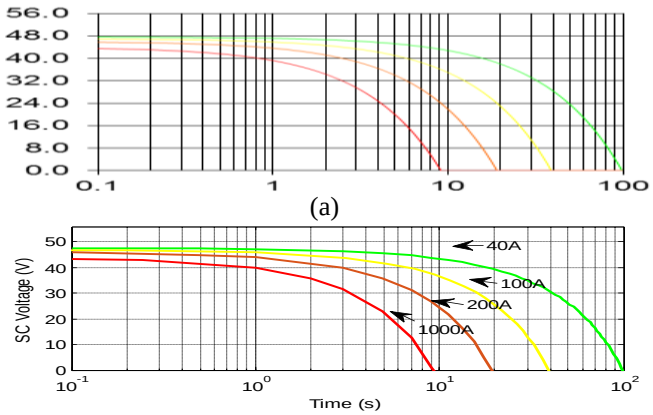

Fig. 7. Current discharge profiles (a) data sheet profiles, (b) simulated profiles.

1) The first control unit MPPT

This control unit is used to maintain the output power of the PV as maximum as possible. This control unit includes 1) modified P&O MPPT and 2) FLC based MPPT algorithms as following:

1) Modified P&O algorithm:

In this method the PV characteristics are measured (I_{pv}, V_{pv} and P_{pv}), and the operating voltage (V_{pv}) is increased (perturbed) by a small decrease (dD) in the duty cycle of the boost converter and observing the change in power divided by the change in current (dP/dI), (but in conventional P&O the PV operating voltage is perturbed and (dP/dV) is observed [6,7]). If (dP/dI) is negative the perturbation of the operating voltage will be in the same direction of increasing so that still decrease the duty cycle of the boost converter. If (dP/dI) is positive the operating voltage should be perturbed in the opposite direction (decreased). The maximum power point is obtained when (dP/dI = 0). The flowchart of this algorithm is shown in Fig. 8.

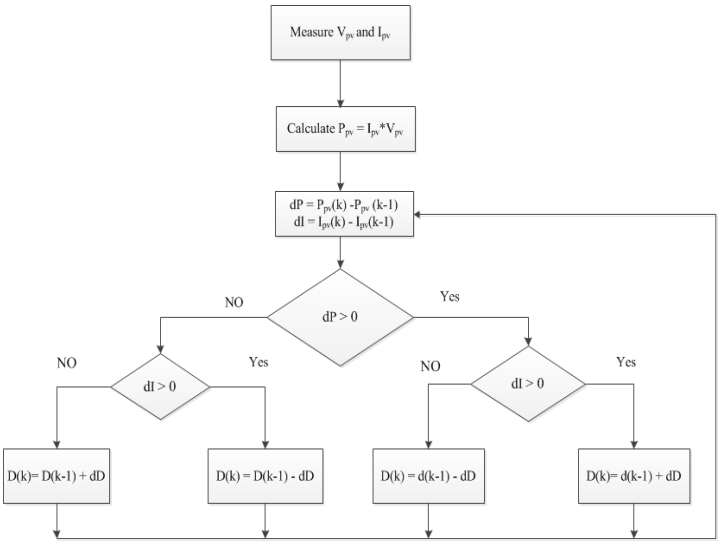

Fig. 8. Modified Perturb and Observe algorithm (P&O).

ISSN:2319-6890)(online),2347-5013(print)
01 August 2015

2)FLC based MPPT algorithm.

This algorithm is based on fuzzifying the Perturb and observe algorithm [8]. The fuzzy logic controller consists of three functional blocks: fuzzification, Fuzzy rules and inference engine, and finally Defuzzification.

- *Fuzzification*

The inputs and outputs of fuzzy must be expressed in linguistic variables to build the fuzzy rules. The input variables of FLC are dP and dI

$$dP = P_{pv}(k) - P_{pv}(k-1) \quad (11)$$

$$dI = I_{pv}(k) - I_{pv}(k-1) \quad (12)$$

The output variable is dD

$$dD = D(k) - D(k-1) \quad (13)$$

Where dP is change in PV power, dI is the change in PV current and dD change in duty cycle of the boost converter. Fig. 9 shows the memberships function of input and output fuzzy sets. Each fuzzy set has four membership functions as following {PB (Positive Big), PS (Positive Small), NS (Negative Small) and NB (Negative Big)}.

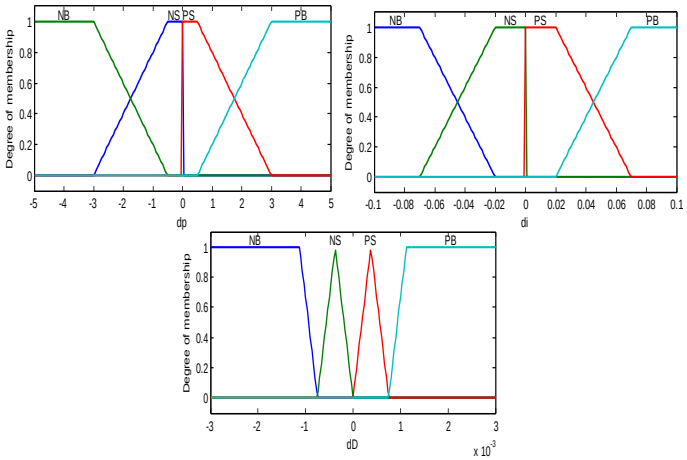

Fig. 9. Input and output fuzzy sets.

- *Fuzzy rules and inference engine*

Fuzzy inference is the process of formulating the mapping from a given input to an output using fuzzy logic. The fuzzy logic rules are 16 rules as in TABLE 2.

TABLE 2. FUZZY RULES

dP \ dI	PB	PS	NS	NB
PB	PB	PB	NB	NB
PS	PS	PS	NS	NS
NS	NS	NS	PS	PS
NB	NB	NB	PB	PB

- *Defuzzification*

The process of Defuzzification calculates the crisp output of the FLC. In this paper the center of gravity method is adopted. The FLC have multiple degrees of freedom to compute duty cycles of different values to track the MPP rapidly with small oscillations.

2) The second control unit.

The second control unit is the energy management controller. It is responsible for stabilizing the output voltage at the reference voltage (V_{ref}) and charging or discharging the energy storage systems. It consists of one outer voltage control loop and two inner current control loops. The first current control loop is to control the charging or discharging current of the battery. The second current control loop is to control charging or discharging current of the SC; According to the load demand and the environmental conditions which effects on the PV output power. Fig. 10 shows the proposed energy management controller which used in the second control unit to control the bidirectional converters to charge and discharge energy storage units and stabilizes the output voltage at the reference voltage. The parameters of the PI controllers which used to control the battery and SC converters are obtained by using try and error method.

The SC charges when the voltage of the DC bus (Vact) is increased suddenly than Vref, to absorb the transient voltage. In this case the SC bidirectional converter operates in a buck mode and sw4 is conducting and charges the SC. When the voltage becomes stable the battery is charged and the bidirectional converter of the battery works in buck mode by conducting SW2. At steady state SC go out and didn't charge or discharge. When the voltage of the dc bus suddenly drops below V_{ref}; the SC will discharge rapidly to compensate the voltage drop and supply the load with the needed power. When the output voltage reaches to its steady state the battery will supply the load. In this case the converter of the battery operates in boost mode by conducting SW3. The SC did not supply the load until the following transient conditions. In this case of discharging; the bidirectional converter works as boost converter and sw5 is conducting. This control strategy will decrease the stress on the battery and hence will increase the life time of the battery. Simulation results will clarify and prove this explanation.

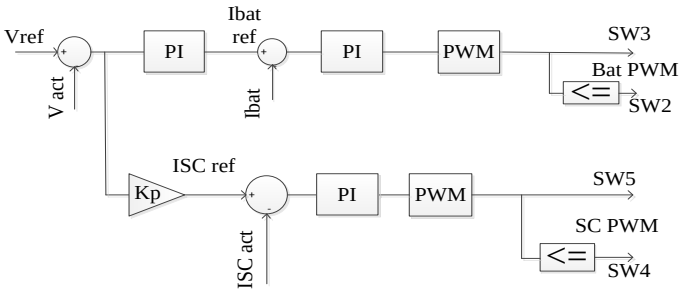

Fig. 10. Proposed energy management controller.

ISSN:2319-6890)(online),2347-5013(print)
01 August 2015

V. Simulation Results

The proposed control strategy can be verified for the following cases: A) Shadow occurs on the PV source when the load is constant, B) The insolation is Constant and step change in load demand, these cases are studied at three different configurations of the system 1) PV only without energy storage, 2) PV with battery, and 3) PV with battery and supercapacitor. The two cases are studied using fuzzy MPPT and modified P&O MPPT techniques to show the performances of the system with the two MPPT techniques.

CaseA: shadow occurs on the PV module and the load Constant at 5A .

In this case the load absorbs a fixed current 5A. Initially the insolation equals to 1000 w/m^2 and T = 25^{o}C then a shadow of 300w/m^2 occurs suddenly on a third of the PV module at t=1 sec. this case were studied by using the two techniques of MPPT. Three configurations of the system are studied under this case to decrease this fault effect as following:

Config1: PV without energy storage.

In this confguration the grid consists of a PV source with the boost converter and the MPPT controller without energy storage. In this configuration all the extracted power from the PV source must be absorbed by the load. From Fig. 11,12 (b) we note that the output power of the PV source initially equals to the maximum power (300 watt) at constant insolation G= 1000 W/m^2, T =25 ^{o}C. The load power equals to PV power 300 W. Suddenly a shadow occurs at time = 4 sec the load voltage drops from 58 V to 36 V. Also the power of the PV module and the load power drops from 300 W to 193 W. The load voltage and the load power are unregulated at constant output voltage, but they varied according to the environmental conditions and the load demand; because there is neither controller on the output voltage nor storage systems to substitute the shortage in power or absorb the surplus PV power. Figs. 11 (a), (b) show the load voltage and the load power and PV power by using FLC MPPT. Figs. 12 (a), (b) show the load voltage and load power and PV power. From these figures we can notice that fuzzy MPPT can reach the MPP faster than modified P&O with low oscillations. Fuzzy reaches to V_{mpp} at t = 0.065 second while modified P&O reaches to V_{mpp} at t = 0.127 second.

Config2: PV with battery.

This configuration integrates the PV source with battery pack. The output voltage controlled by using the proposed energy management controller. In this configuration the load power equals to 250 W and the output voltage is controlled at 50 V.
Initially the solar insolation G= 1000 W/m^2 and T= 25^{o}C. The maximum PV output power tracked using FLC algorithm as shown in Fig. 13, and by using modified P&O algorithm as shown in Fig. 14. The available maximum output power from the PV = 300 W is larger than the load power = 250 W so that the battery is charging with surplus power from the PV = 50 W. Suddenly a shadow 300 w/m^2 occurs at time = 4 sec on a third of the PV module. The PV power drops from 300 watt to100 watt then oscillates around 193.4 watt, which is the global MPP (GMPP) as shown in Fig. 13(b). The oscillations when using fuzzy is smaller than using modified P&O as shown in Figs 13, 14.

Config3: PV with battery and SC.

This configuration integrates the PV source with battery pack and SC. The output voltage controlled by using the proposed energy management controller. In this case the load absorbs 250 W and the output voltage is controlled at 50 volt.
Initially the solar insolation G= 1000 w/m^2 and T= 25^{o}C. The maximum PV output power tracked using FLC as shown in Fig. 15, and by using modified P&O as shown in Fig. 16. The available maximum output power from the PV = 300 W is larger than the load power = 250 W. At starting time the SC will provide power to the load and the battery to stabilize the output voltage at reference voltage and to decrease the transient voltage drop until the battery reaches to its steady state charging current and goes out as shown in Fig. 15 (b). Suddenly a shadow 300 W/m^2 occurs at time = 4 sec on a third of the PV module. The PV power drops from 300 W to 100 watt, which is the local MPP, then back to 193.4 watt which is the global MPP as shown in Figs. 15, 16(b). At this instant the SC will discharge rapidly to substitute the shortage in load power, until the battery reaches to its steady state of discharging, and then the SC didn't supply power. This strategy decreases the stress on the battery and allows the internal chemical reactions to occur safely. These results show that FLC MPPT reduces oscillations around the MPP and fast to track the global maximum power point.

CaseB: Insolation constant and step change in the load demand.

In this case the solar insolation is constant at 1000 w/m^2 and T=25^{o}C. The load current changes from 7A to 4 A at time = 4 sec. in this case we will study the performance of the system with three configurations as the previous case as following

Config1: PV without energy storage.

In this confguration the grid consists of a PV source and the MPPT controller without energy storage. In this configuration all the extracted power from the PV source must be absorbed by the load. Initially the output power of the PV source equals to the maximum power (300 W) at constant insolation G = 1000 W/m^2 and T =25 ^{o}C. The load power equals to PV power = 300 W as shown in Figs. 17, 18(b). Suddenly the load current drops from 7 A to 4 A at time = 4 sec, the output voltage increases from 42.8 V to 75 V. The Output power and the load power still constant at MPP. The load voltage and the load power are unregulated at constant output voltage, but they varied according to the environmental conditions and the load current; because there is neither voltage controller on the output voltage nor energy storage systems to substitute the shortage in power. Figs. 17(a), (b) show the load voltage and the load power and PV power by using FLC MPPT. Also Figs. 18(a), (b) show the load voltage and load power and PV power respectively using modified P&O MPPT. From these figures we can notice that FLC MPPT can reach the MPP faster than modified P&O and with lower oscillations.

ISSN:2319-6890)(online),2347-5013(print)
01 August 2015

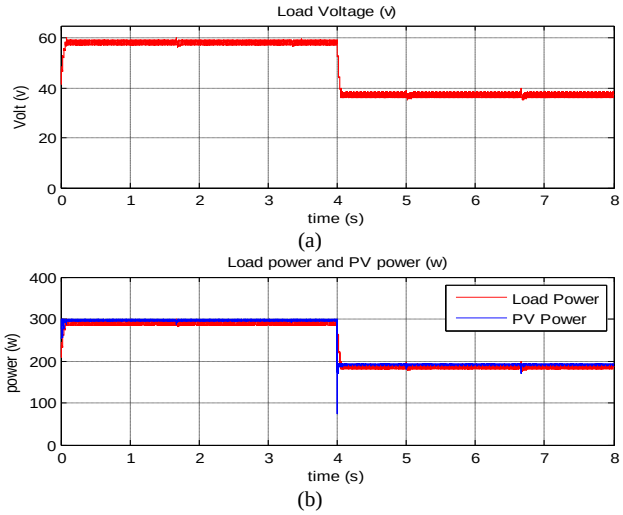

Fig. 11. Case (A) config1 using FLC MPPT a) load voltage , b) load power and PV power.

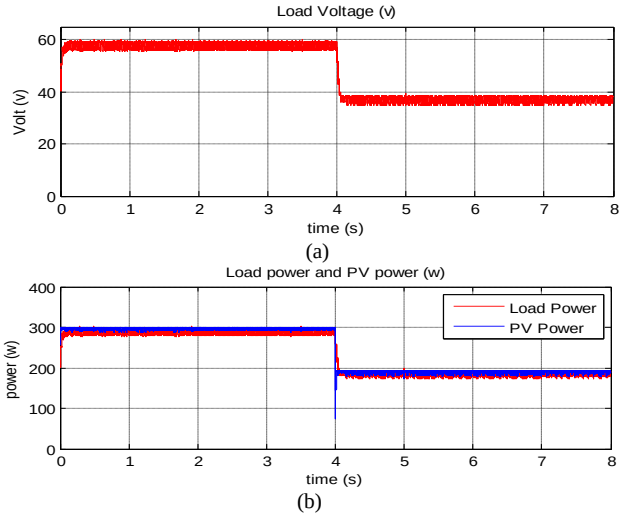

Fig. 12. Case (A) config1 using modified P&O MPPT a) load voltage, b) load power and PV power.

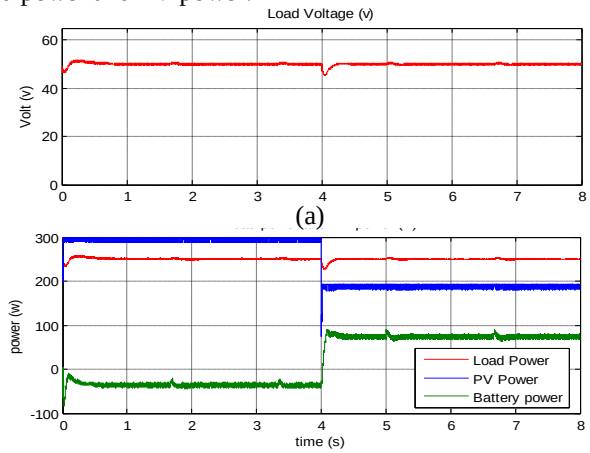

Fig. 13. Case (A) config2 using FLC MPPT. (a) load voltage, (b) load power and PV power.

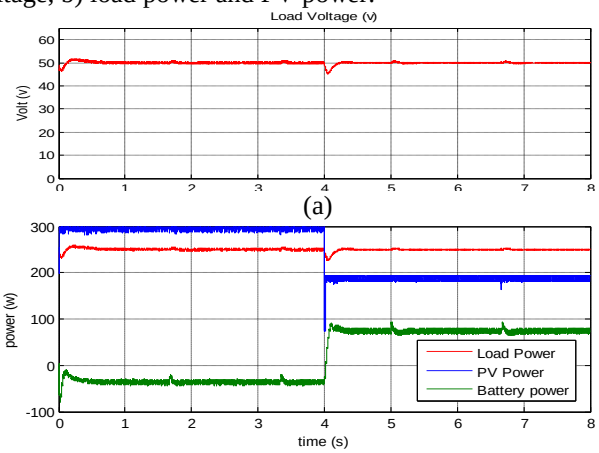

Fig. 14. Case (A) config2 using modified P&O MPPT (a) load voltage, (b) load power and PV power.

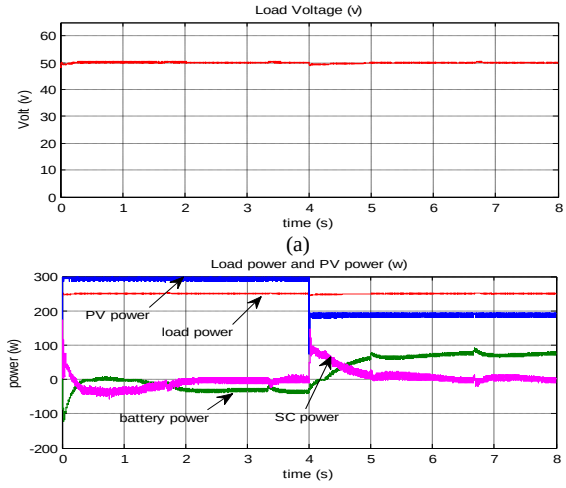

Fig. 15. Case (A) config3 using FLC MPPT. (a) load voltage, (b) load power, PV power, battery power and SC power.

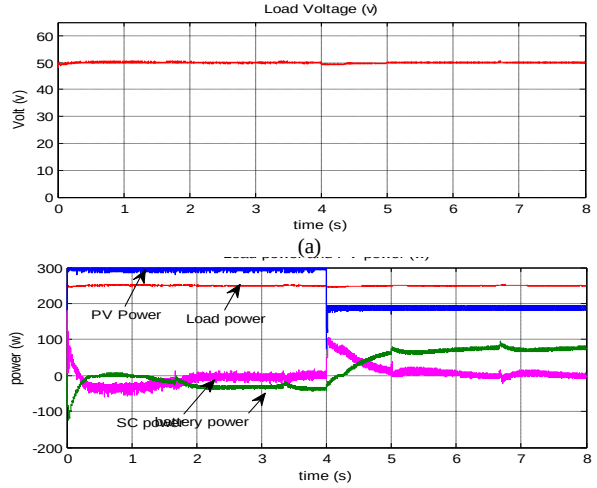

Fig. 16. Case (A) config3 using modified P&O MPPT. (a) load voltage, (b) load power, PV power, battery power and SC power.

ISSN:2319-6890)(online),2347-5013(print)
01 August 2015

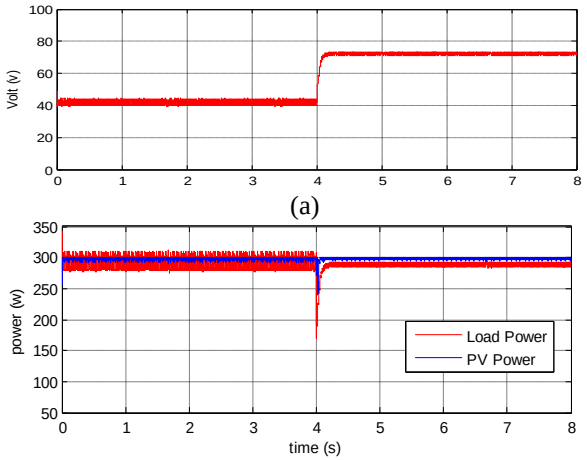

Fig. 17. Case (B) config1 using FLC MPPT (a) Load voltage, (b) Load power and PV power.

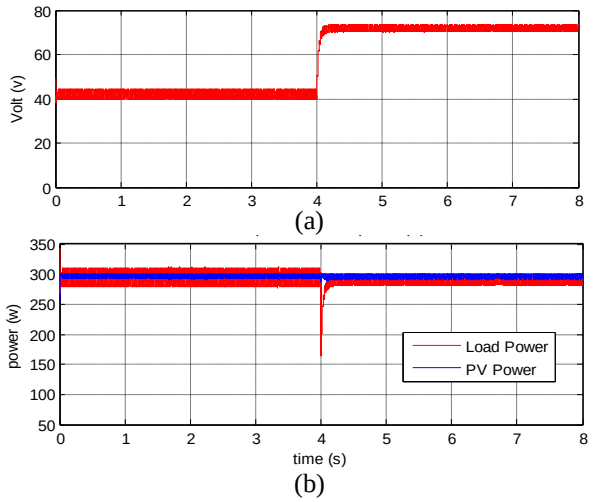

Fig. 18. Case (B) config1 using modified P&O MPPT (a) Load voltage, (b) Load power and PV power.

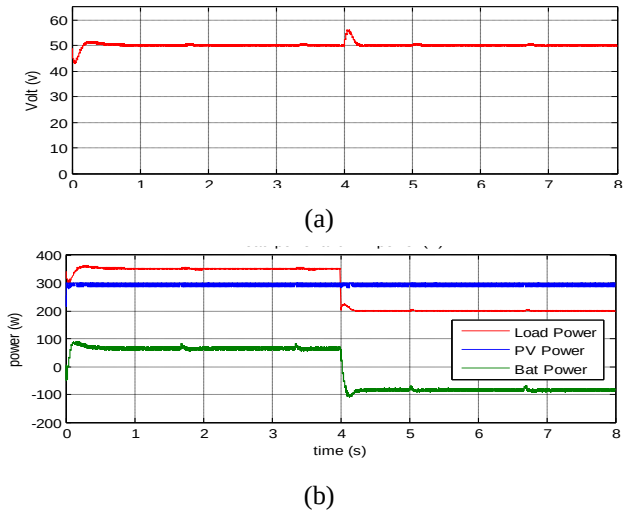

Fig. 19. Case (B) config2 using FLC MPPT (a) load voltage, (b) load power, PV power, and battery power.

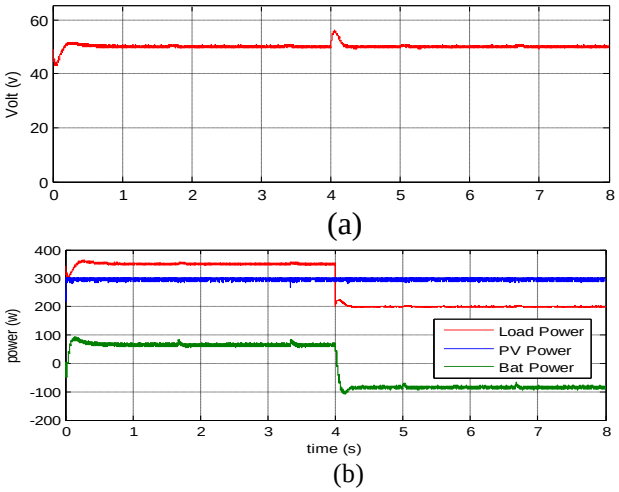

Fig. 20. Case (B) config2 using modified P&O MPPT (a)load voltage, (b) load power, PV power, and battery power.

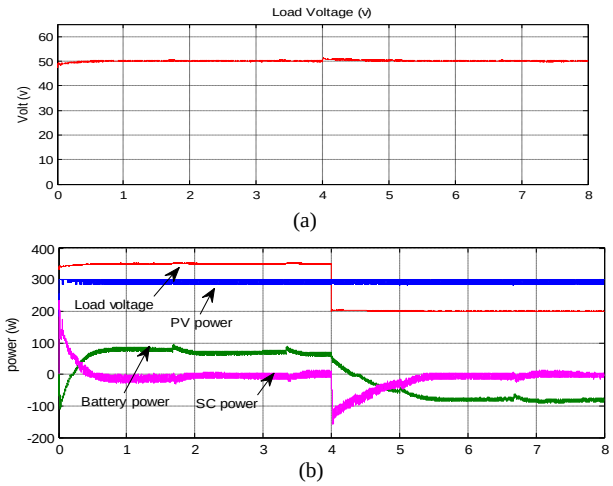

Fig. 21. Case (B) config3 using FLC MPPT (a)load voltage, (b) load power, PV power, battery power and SC power.

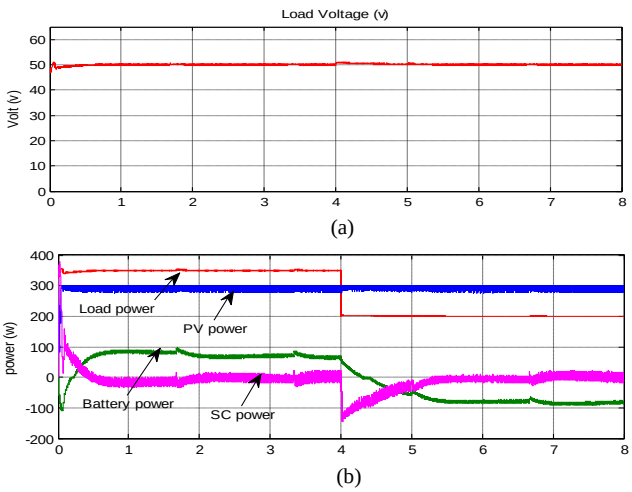

Fig. 22. Case (B) config3 using modified P&O MPPT (a)load voltage, (b) load power, PV power, battery power and SC power.

ISSN:2319-6890)(online),2347-5013(print)
01 August 2015

Config2: PV with battery.

In this configuration the battery used as the energy storage source to store the surplus power from the PV source. The output voltage controlled by using the proposed energy management controller at V_{ref} = 50 V. Initially the load power = 350 W and the output voltage is controlled at 50 V, at constant G = 1000 W/m^2 and T= 25^{o}C. The maximum PV output power tracked using FLC algorithm as shown in Fig. 19, and by using modified P&O algorithm as shown in Fig. 20. The available maximum output power from the PV = 300 W is lower than the load power = 350 W so that the battery is discharging to substitute the shortage in PV power = 50 W . Suddenly the load demand drops to 200 W at time = 4 sec. The excess in PV power 100 W will be supplied to the battery (charging the battery) as shown in Figs 19, 20 (b). The simulation results show that the battery is forced to be charged and discharged rapidly which affected badly on its life time. Also using FLC MPPT can reach the MPP faster than modified P&O with low oscillations.

Config 3: PV with battery and SC.

This configuration integrates the PV source with battery and SC. The output voltage controlled by using the proposed energy management controller. Initially the load absorbs 350 W and the output voltage is controlled at V_{ref} = 50 V. The maximum PV output power tracked at solar insolation G= 1000 W/m^2 and T= 25^{o}C using FLC as shown in Fig. 21, and by using modified P&O as shown in Fig. 22. The available maximum output power from the PV = 300 W is smaller than the load power = 350 W. At starting time the SC will provide power to the load and the battery to stabilize the output voltage at reference voltage and to decrease the transient voltage drop until the battery reaches to its steady state discharging current and SC goes out as shown in Figs. 21, 22(b). Suddenly a step decrease in load power at time = 4 sec from 350 W to 200 W. So that the SC charges immediately to absorb the surplus power from the PV source to maintain the output voltage at V_{ref} until the battery reaches to its steady state charging current. Then the SC goes out (did not charge). When we comparing between config3 and config2 from Figs. 19, 20, 21, 22 it can be noticed that the voltage change in config3 is smaller than voltage change in config2 and the battery charges or discharges without stress which increase its life time.

VI. Experimental Case Study

Maximum power point tracking and energy management is experimentally verified in a micro grid system. The system consists of three lead acid deep cycle batteries 12 volt 50 Ah, A boost converter, PLZ1004W DC electronic load, and a PV module IS4000P similar to the unit in Fig. 23 placed on the roof top of the electronics research institute at Giza Egypt. The experimental setup of the system is shown in Fig. 23. The modified P&O MPPT algorithm is experimentally validated using digital signal processing card (DSP1102). The program is built using MATLAB Simulink. The experimental results show that the output power is kept at the available maximum power point of the PV module in all cases. In Fig. 24 the available maximum PV power = 113 W , maximum current = 3.63 A, and the PV voltage = 31.12V. These values at the input side of the boost converter. At the output side of the boost converter maximum power = 101.7W because there is 10% losses in the boost converter. The output current from the boost converter = output power (101.7) / output voltage (38.5) = 2.64 A. At the first period from 0 sec to 18 sec, the load current = 3 A, so that the battery discharges by = 3 - 2.64 = 0.4A. at the second period from time 18 sec to 47 sec the load disconnected and the battery absorbs all the output current = 2.64A. At the third period from 47 sec to 60 sec the load reconnected again and absorbs 0.48A, but the voltage of the battery bank increased to 44 volt so that the battery absorbs 1.81A. In all cases the out power from the PV still at the maximum available power

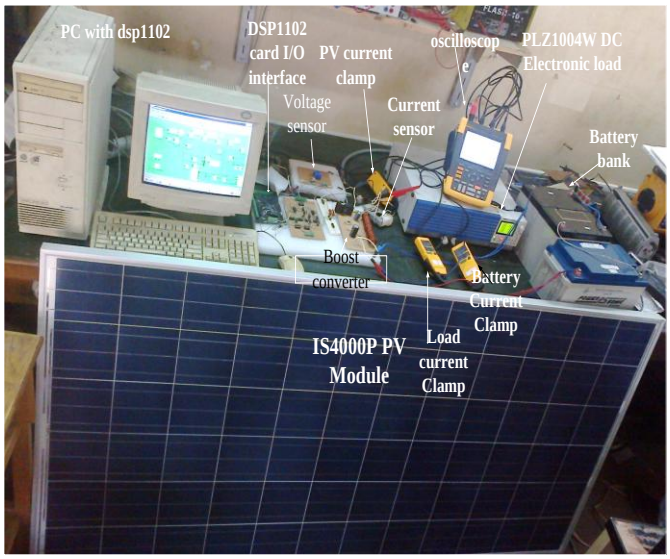

Fig. 23. Experimental setup

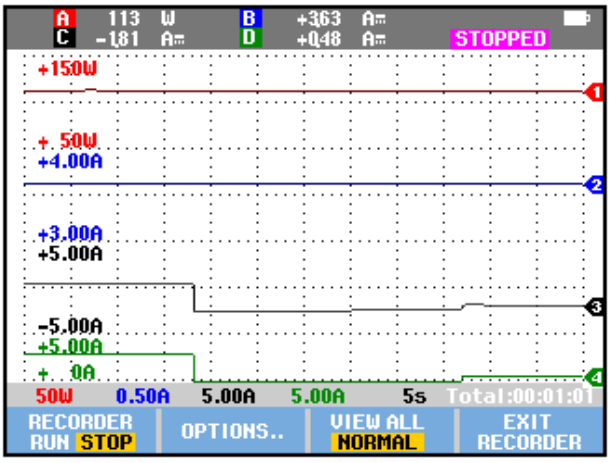

Fig. 24. Experimental results: PV Power on ch (A), PV current on ch (B), battery current on ch (C), and load current on ch (D)

ISSN:2319-6890)(online),2347-5013(print)
01 August 2015

VII. CONCLUSION

The modeling and simulation of each element of a micro grid has been introduced. A smart energy management control strategy has been proposed. A modified method for P&O has been introduced taking the change of current instead of the change in voltage. This modified method increased the sensitivity of MPPT especially at partial shadowing faults. The method compared with FLC based MPPT. From the simulation results it can be noticed that FLC is faster and has lower oscillations around the maximum power than the modified P&O. Different configurations of the micro grid have been studied with the proposed energy management controller. The simulation results show that the configuration which integrates the PV source with battery and SC is the best configuration. Because the stress on the battery is decreased which increase the life time of the battery. Also the amplitude of the voltage change has been decreased in this configuration because of fast charging and discharging of the SC and its high power density. An experimental case study has been executed. The results show the effectiveness of the modified P&O MPPT to maintain the operating point at the available maximum power at different cases of load demand.

• REFERENCES

i. *Navid Eghtedarpour, Ebrahim Farjah, "Distributed charge/discharge control of energy storages in a renewable-energy-based DC micro-grid," IET Renewable Power Generation , Vol. 8 , Issue. 1, pp. 45-57, 2014.*

ii. *F. D. Kanellos, A. I. Tsouchnikas, N. D. Hatziargyriou, "Micro-Grid Simulation during Grid-Connected and Islanded Modes of Operation," International Conference on Power Systems Transients (IPST'05), Canada, June 19-23, 2005*

iii. *M.E. Glavin, Paul K.W. Chan, S. Armstrong, and W.G Hurley, "A Stand-alone Photovoltaic SupercapacitorBattery Hybrid Energy Storage System," IEEE 13th Power Electronics and Motion Control Conference, pp. 1688 – 1695, 1-3 Sept. 2008 .*

iv. *A.Z. Annuar, A.H.M. Yatim, "A Development of Fuzzy Control of Hybrid Energy System using Ultracapacitor," 2nd IEEE International Conference on Power and Energy (PECon 08), December 1-3, 2008, Johor Baharu, Malaysia.*

v. *W. Li, G. Joós, "A Power Electronic Interface for a Battery Supercapacitor Hybrid Energy Storage System for Wind Applications," IEEE annual power electronics specialists conference PESC , pp. 1762 - 1768 , 2008.*

vi. *V. Salas, E. Olias, A. Barrado, A. Lazaro, "Review of the maximum power point tracking algorithms for stand-alone photovoltaic systems," Solar Energy Materials & Solar Cells, pp.1555–1578, 2006.*

vii. *Dalila BERIBER,"MPPT Techniques for PV Systems," 4th International Conference on Power Engineering, Energy and Electrical Drives.*

viii. *B. N. Alajmi, K. H. Ahmed, S. J. Finney, and B. W. Williams, "Fuzzy-Logic-Control Approach of a Modified Hill-Climbing Method for Maximum Power Point in Microgrid Standalone Photovoltaic System," IEEE Transactions on Power Electronics, vol. 26, no. 4, April 2011.*

ix. *Atef .M. Mansour, Khaled .N. Salama, Essam Abu Elzahab,"Fault Diagnosis of PV-System in a Smart Grid Using Fuzzy Logic Classifier," 3rd International Conference on Advanced Control Circuits and Systems (ACCS'013),30 Nov. – 03 Dec. 2013, Luxor, Egypt*

x. *O. Tremblay, L.A. Dessaint, A. Dekkiche, "A Generic Battery Model for the Dynamic Simulation of Hybrid Electric Vehicles," IEEE Vehicle Power and Propulsion Conference VPPC 2007, pp. 284-289, 9-12 Sept. 2007.*

xi. *S. N. Motapon, L. A. Dessaint, and K. Al-Haddad,"A Comparative Study of Energy Management Schemes for a Fuel-Cell Hybrid Emergency Power System of More-Electric Aircraft," IEEE Transactions on industerial electronics, vol. 61, no. 3, pp. 1320-1334, March 2014.*